

Surface-Tension Induced Convection at Reduced Gravity

Simon Ostrach* and Avind Pradhan†
Case Western Reserve University, Cleveland, Ohio

Fluid motions are induced by surface-tension gradients on the free surface of a liquid in a cylindrical container which is in free fall in a drop tower. Identical experiments are conducted in a normal gravitational environment. The motion in that case is due to natural convection. The ratio of surface-tension to buoyancy forces in the tests is of the order of 10^4 at reduced gravity conditions and 0.13 under normal gravity. In each case a two-way flow occurs throughout most of the liquid. Comparison of the results from the two types of experiments is made in order to indicate differences in the flow details.

Introduction

THERE are a variety of nongravity forces, as well as gravity itself, that can induce fluid flows in space. Such nongravity driving forces include surface or interfacial tension, g-jitter, thermal volume expansions, and magnetic and electric fields.

The present experiments are directed to examine one of the aforementioned driving forces, viz., surface-tension gradients. The objective of the research is to study the surface-tension induced convection under reduced gravity and to compare it with normal gravity convection with all other conditions identical. The intensities of such flows and their penetration depth below the free surface are also determined. In this way the dominant role of a free surface in a reduced-gravity environment is indicated.

The interface between two fluid phases can influence the motion of fluids when either the interface has finite curvature or when the interfacial tension varies from point to point. In both cases forces appear in the interfacial region that can affect or generate fluid motions.

The relative importance of surface-tension and gravitational forces is usually estimated from the Bond number, $B_0 = \rho g L^2 / \sigma$, where ρ is the fluid density, g the acceleration of gravity, L a characteristic dimension, and σ is the surface tension. From the Bond number it is clear that, on Earth, surface tension is important (Bond number less than unity) only in small-scale configurations, i.e., where L is small. Therefore, most existing work on the effect of surface tension deals with flows in capillaries and thin films or the motion of droplets or bubbles or short wavelength water waves. In space, on the other hand, surface tension becomes a significant force whose influence on fluid motion must be assessed and understood.

Surface-tension gradients can arise from gradients in temperature or concentration. These surface-tension gradients can generate conventional convection flows or cellular flows just as gravity induces those two types of natural-convection flows. When the surface-tension gradients and density differences are due to temperature gradients the dimensionless parameter related to gravitational convection is the Grashof number, $Gr = \beta g \theta L^3 / \nu^2$ and the corresponding

one for surface-tension induced flows is the Marangoni number, $Ma = (\partial \sigma / \partial T) \theta L / \rho \nu \kappa$, where β is the fluid volumetric expansion coefficient, θ is a characteristic temperature difference, T is the fluid temperature, ν is the kinematic viscosity, and κ is the thermal diffusivity. Note that the Marangoni number is independent of gravity. The relative magnitude of surface tension and buoyancy forces is given by the ratio $Ma/Gr = \nu (\partial \sigma / \partial T) / \rho \beta g L^2 \kappa$, which is the reciprocal of a modified Bond number. The experiment is designed so that this ratio (Ma/Gr) takes on values from about 0.13 to 1.5×10^4 in normal and reduced-gravity environments, respectively.

There are many possible modes of flow and configurations of interest in which the surface tension can be significant. The particular situation focused on herein is the role of the free surface on reduced-gravity convection. Under appropriate conditions the flow and heat transfer of a fluid in an open container can be expected to change significantly as gravity is reduced. For example, in a normal gravitational environment the natural convection (due to buoyancy) may be turbulent. In a somewhat reduced-gravitational environment the gravity force may still predominate over the surface tension, but the natural convection could be quite different, i.e., it could be laminar, cellular, or both. In these cases the free surface can be said to be passive with respect to the convection in the sense that the fluid motion is induced by buoyancy. However, as gravity is reduced further the surface-tension gradient force becomes dominant and will generate the primary fluid motion. In such a case the free surface becomes an active factor in the convection process.

Among the existing publications related to this problem are the ones reported in Refs. 1 to 4. Babskiy et al.¹ give consideration to the steady flow generated by the free surface in a rectangular enclosure in which the two opposite walls that bound the free surface are at different temperatures. It is indicated that the solutions are valid for "sufficiently small" Marangoni numbers (~ 1.0) yet results are presented for values of this parameter of 5 and 500. An exact solution is found by Birikh² for the equations for free convection and surface tension in an infinite plane-parallel horizontal layer of liquid with a constant temperature gradient in the horizontal direction. Here also the steady state has been considered. Levich³ has discussed purely capillary convection. Yih⁴ has pointed out many inconsistencies in his solution and has given a corrected solution of the Levich problem.

The only reduced gravity experiments on surface-tension driven flows are those induced by a thermal instability⁵ (heating from below) and, thus, are different from the configuration of interest herein. Since there did not appear to be any experimental study of conventional convection due to surface tension alone, the present experiments were developed to be conducted in the NASA Lewis Research Center's 500-ft drop tower in which approximately 5.5 s of reduced gravity

Presented as Paper 77-118 at the AIAA 15th Aerospace Sciences Meeting, Los Angeles, Calif., Jan. 24-26, 1977; submitted Feb. 1, 1977; revision received Dec. 14, 1977. Copyright © American Institute of Aeronautics and Astronautics, Inc., 1977. All rights reserved.

Index categories: Boundary Layers and Convective Heat Transfer—Laminar; Space Processing.

*Wilbert J. Austin Distinguished Professor of Engineering, Department of Mechanical and Aerospace Engineering. Fellow AIAA.

†Graduate Assistant.

(about $10^{-5} g_0$) can be obtained. From an order of magnitude analysis⁶ it was estimated that it would take somewhat less than 3 s for the surface boundary layer to reach steady state. Thus, worthwhile data could be obtained in that facility.

Experimental Setup

The drop tower facility imposed a number of constraints on the test apparatus. The size is limited by that of the drop module and the instrumentation and power supply have to conform to the capsule capacity. In addition, it must be able to withstand the impact of a 40-g deceleration. The test apparatus mounted in a plexiglass leakproof chamber that is maintained at a pressure of 1 atm, even when the drop-tower pressure is 100 μ of mercury, is shown in Fig. 1. The liquid container is a cylindrical plexiglass dish with a 10-cm i.d. and 3.0-mm thick vertical walls. The inner wall of the dish is covered with a teflon tape (0.2-mm thick) to yield a 90-deg contact angle with distilled water at 25°C. Considerable preliminary testing⁶ was required to determine this method of maintaining a flat interface and preventing creeping of liquid up the walls at reduced gravity.

Distilled water is chosen as the test fluid because it had the following properties: 1) large surface-tension variation with temperature, 2) low viscosity, 3) small density variation with temperature, 4) transparency, and 5) easy accessibility. The temperature gradient is imposed by an infrared heat source located above the free surface (see Fig. 1). This 80-W heater is 3.5-cm long with a 0.635-cm diameter. It is made by wrapping 30-cm long Ni-chrome wire, 0.27- μ in diameter over a 3.2-mm-o.d. single hole ceramic tube for a length of 3.2 cm. It is insulated by coating it with creamy insulating high-temperature cement. This configuration when still wet is carefully slipped inside a 0.6-mm-i.d. and 0.635-cm-o.d. steel tube which serves as a casing. More cement is inserted into the tube for better packing and closing the two ends. To dry the cement the heater is placed into a dryer. The heater has a resistance of 5.0 Ω and operates on a 4.0-A supply.

The heat source is positioned vertically above the liquid at the center of the dish with its bottom 2.5 mm \pm 0.05 mm above the free surface. With such a heating from above configuration, convection due to buoyancy is minimized and the temperature gradient on the free surface is imposed faster than by heating the side wall.

Methylene blue dye is used to make the flow patterns visible. Four 40-mesh dye particles and $\frac{1}{2}$ mg of fine ground (400-mesh) dye are placed on top of a knurled spoon which, when vibrated by means of a 24-V dc motor, sprinkles the dye on the liquid free surface about 10 s before the start of the test. Some of the finely ground dye spreads over the free surface and the larger dye particles penetrate into the liquid and form vertical strands. When the fluid is completely

stationary and there are no temperature gradients, the dye strands maintain their position and do not diffuse for about a minute. When the test starts and the liquid moves, the dye strands also move and thereby indicate the velocity profiles. Top and side views of the dish are recorded on movie film by two 16-mm high-speed Melikon cameras that are mounted as shown in Fig. 2.

The leakproof enclosure as shown in Fig. 1 is made of 20.32-cm-i.d. and 21.59-cm-o.d. cylindrical plexiglass tube. The height of the cylinder between the top and bottom plates is 10.795 cm. An O-ring groove 22.225-cm normal diameter and 0.3175-cm thick is cut at the bottom of the cylinder so that the O-ring seals the cylinder.

To measure the radial surface temperature gradient imposed by the heat source, five thermistor probes (accuracy $\pm 1^\circ\text{C}$) are placed so that their beads just touch the free surface. The thermistors are attached to the amplifier transmitter and other electronic circuitry for the transmission of temperature data to the control room where the output load voltage at each thermistor probe is recorded on a strip chart as a function of time. This output load voltage is converted to temperature using calibration curves. (See Ref. 6 for more details.) To avoid any disturbance on the free surface due to other than 90-deg contact angle between probes and water, a shrinkable teflon tube is slipped over the probes. However, two kinds of disturbances are noticed on the free surface and are attributed to the presence of the thermistors. The first kind of disturbance stays around the thermistors and is due to the thermistors not being exactly vertical. This leads to the interface not being flat around the thermistor probes. The second kind of disturbance is a standing wave (amplitude ~ 0.1 mm) which starts from the thermistor probes. The beads are never seen to come out of the free surface. Running the data film at slow speed, it is noticed that the cantilever on which probes are mounted oscillates as the capsule goes into reduced gravity due to loss of weight and spring back action.

For the preceding reasons some velocity data are taken without the thermistors in place in order to eliminate disturbances due to the thermistors. The previous temperature profile readings are considered to be applicable for these tests as well. This is true because the disturbance is small and so there is little particle motion as such, which would lead to small heat transfer. The temperature measurements are made once the waves subsided about 1 s after the release of the module in the drop tower. The disturbances caused by thermistor probes presumably change the temperature field, but no accurate estimate can be made of the error caused by it.

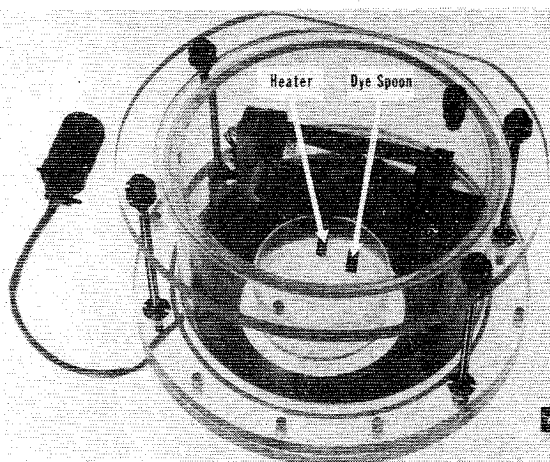


Fig. 1 Test container.

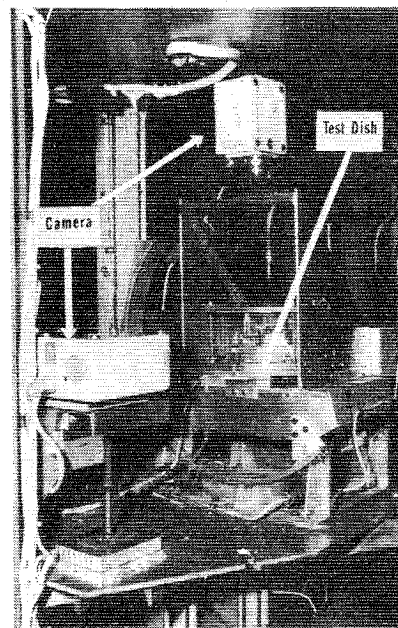


Fig. 2 Apparatus in drop module.

Table 1 Average values of relevant dimensionless parameters^a

	Reduced gravity		Normal gravity	
	After 3 s of heating	After 5 s of heating	After 3 s of heating	After 5 s of heating
<i>Ma</i>	6.43×10^4 (1.57×10^5)	1.66×10^5 (3.61×10^5)	6.05×10^4 (3.43×10^5)	1.116×10^5 (7.52×10^5)
<i>Gr</i>	4.497 (11.0)	2.54 (27.3)	4.097×10^5 (2.33×10^6)	8.58×10^5 (5.78×10^6)
<i>Ra</i>	24.40 (59.68)	65.77 (143.18)	2.26×10^6 (1.285×10^7)	4.5×10^6 (3.03×10^7)
<i>Ma/Gr</i>	1.48×10^4	1.32×10^4	0.1476	0.130

^a Values in parentheses are the maximum values. The average values are calculated using the average surface temperature and temperature differences. The maximum values are calculated using the maximum surface temperatures and maximum temperature differences. All values are for a 80-W infrared heating source.

Two electronic clocks, which are visible in the films, are used to record time. The clocks are connected to the heater solenoid so that time is measured from the moment the heater comes to position above the free surface. Both clocks work simultaneously. Error involved in time measurement is 0.01 s.

Experimental Procedure

The dish is first cleaned by a special process (see Ref. 6) to eliminate any possible contamination. The inner wall of the dish is then covered with a single layer of transparent teflon tape. The dish is cleaned again with methyl alcohol and distilled water. The dish is then taped (double-stick tape) into place. The distilled water is added up to the thermistor beads. The heater is adjusted so that when it comes to position, its bottom is 2.5 mm from the free surface.

The particles of methylene blue are carefully placed on the vibrator spoon. The test apparatus is then placed in the leakproof tank which was hydrostatically tested for leaks and found to be good up to a pressure difference of 13 psi, which is considered sufficient for these tests. The entire apparatus is then assembled in the capsule for the drop-tower test. The drop module is hung in the drop tower for 45 min so that the fluid can become stationary before the test.

The following tests are run in the drop tower:

1) The heat source starts heating the free surface 1 s after the package is released.

2) The free surface is preheated for 10 s before the drop.

3) The free surface is preheated for 40 s before the drop.

Test 1 is performed to see how the flow starts with surface tension gradients being dominant. This might also give some idea as to what kind of steady-state flow pattern can be expected for high reciprocal modified Bond number (greater than 10^4) cases. Tests 2 and 3 show any abrupt changes in flows as the gravity level is dropped to $10^{-5} g_0$. All of the tests are performed at normal gravity also, with all initial conditions identical.

Test conditions are initial temperature, 23°C, surface-tension temperature, $d\sigma/dT = 0.16$ dyn/cm/°C, characteristic length of 4.5 cm. The heater is initially heated for about 2 min, 35 s far from the free surface. In this time interval the steady state of the heater is achieved, and it is in this state that the heater is used to heat the free surface. This steady-state time of the heater is measured by means of a thermocouple attached to its lip. Once the calibrations are over, the thermocouple is removed and the heater is heated in all experiments for the same time period (2 min, 35 s). The relevant dimensionless parameters are indicated in Table 1.

Results

The results of the various experiments are presented in the order in which they were described previously.

Test 1

The heat source starts heating the free surface 1 s after the package is released. This 1-s time interval is given to eliminate any small disturbances that are produced by the release mechanism. A previous test under identical conditions has

shown that the disturbance caused by release is very small (amplitude less than 1.0 mm) and lasts for about 0.5 s.

The surface-tension gradient induced motion starts soon after the heater starts to heat the surface as can be seen from the movie frames (see Fig. 3). The flow starts from the center close to the heater and spreads outward as the temperature gradient is established (see Fig. 4). The temperature profiles in Fig. 4 are for a single run and are drawn assuming that the free surface temperature close to the side wall remains the same as the initial liquid temperature in the time interval of 5 s. This is done to get some idea of the characteristic temperature difference. The temperature profiles in Fig. 4 are for a test where the heating starts with the release of the package in the drop tower.

Looking at the movie films, it appears that a very thin film on the surface is pulled away from the heater at considerable speeds because of the induced surface-tension gradient. Very little or no motion could be observed around 3.0 cm away from the center of the dish, where the surface tension gradient is also found to be small. The free surface velocities are shown in Fig. 5 and represent the velocities measured from three runs starting at 2.0 s after heating. As the free surface velocities are measured by tracking the dye particles on the surface, for small velocities like 2.0 mm/s, the dye particle displacement is measured at intervals of 1.0 s. Thus, the velocities shown in Fig. 5 are those measured from a time interval of 2 to 3 s after heating.

As soon as heating starts, the dye movement is observed around the heater, but after 2.0 s of heating all of the free surface is not active. The dye movement is observed only up to a radius of about 2.0 cm from the center, because temperature gradients are established in that region only. However, after 3.0 s of heating almost all of the dye has moved out from the center and no measurements can be made there. Velocities measured about 2.5 cm away from the center are seen to be the same as those shown in Fig. 5.

In the interior of the liquid a two-way motion is observed, i.e., flow away from the heater close to the free surface and the rest of the fluid moving in the reverse direction because of continuity. Representative frames from the movie film are presented in Fig. 6 to show the change in the dye strands with time. Dye strand displacements with time as determined from the films are given in Fig. 7. Before the heat is imposed the dye strands are stationary, although they are not necessarily straight and vertical. If vertical velocities are assumed to be negligible, the dye strand displacements can be used to calculate internal fluid velocities. From these figures it can be seen that a boundary layer forms close to the free surface. Outside this free-surface boundary layer the fluid moves toward the center with a velocity of 1.0 ± 0.2 mm/s.

The $(Ma/Gr)_{avg}$ ratio is found to be around 10^4 (see Table 1) for a given test. The ratio is a function of average liquid temperature and the gravity level. During a specific test its value does not change too much (max. 10%) as the average liquid temperature changes by no more than 10°F in the 5-s time period. The initial liquid temperature being about 80°F, this change in liquid temperature gives rise to only small changes in the constants which form $(Ma/Gr)_{avg}$ ratio. The average liquid temperature at different time intervals is

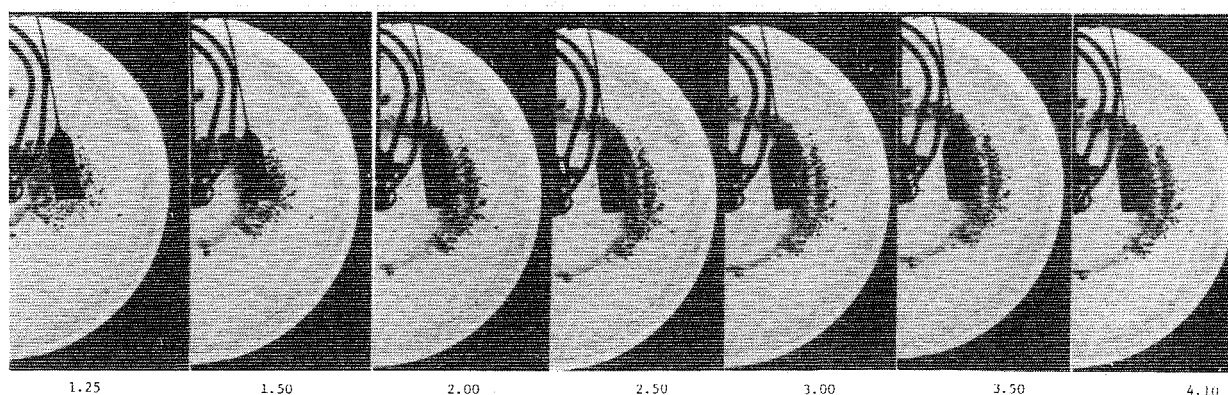


Fig. 3 Test 1: (top view) surface flow at reduced gravity. Surface heating started 1 s after release. Numbers below pictures give the time (in seconds) after release.

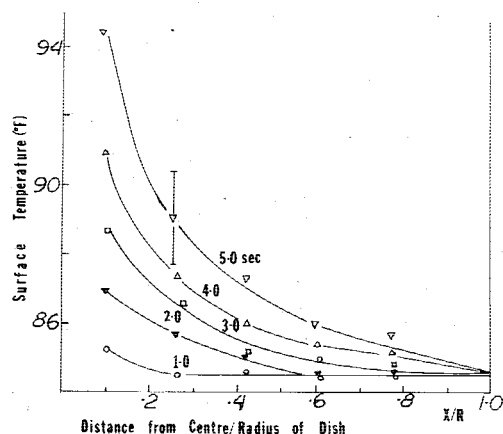


Fig. 4 Surface temperature profiles at reduced gravity.

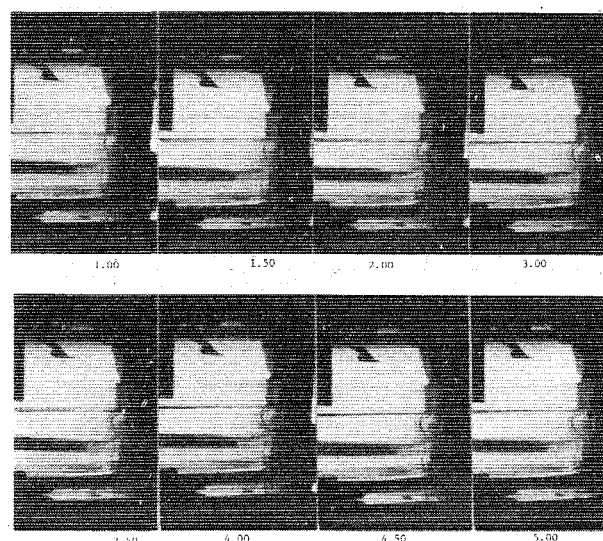


Fig. 6 Test 1: (side view) interior flow at reduced gravity with no preheat.

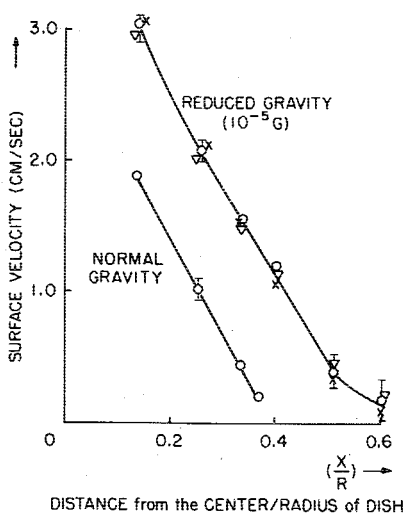


Fig. 5 Surface velocity vs distance from center of dish. Taken 2 s after heating.

calculated using the surface temperature profiles given in Fig. 4 and making use of the following formula:

$$T_{\text{avg}} = \frac{2}{R^2} \int_0^R T(r) r dr$$

where R is the dish radius. As the temperature profiles in Fig. 4 are drawn from a distance of 0.5 cm from the center to the side wall of the dish, the temperature profiles from the center to a radius of 0.5 cm are assumed (for calculation purposes) to be simply the extension of the given profiles and drawn as tangents at $x/R = 0.1$.

The average temperature difference used in the calculation of Marangoni, Grashof, and Rayleigh numbers is as follows:

$$(\Delta T)_{\text{avg}} = T_{\text{avg}} - T_w$$

From the values of dimensionless parameters that are given in Table 1 we see that Marangoni number which represents surface-tension gradient induced flow is about 10^4 times larger under reduced gravity than the Grashof number which represents buoyancy induced flow. This indicates that the flow due to surface-tension gradient is dominant.

As the heating is continued we see that the value of $(Ma/Gr)_{\text{avg}}$ ratio reduced from 1.48×10^4 (at 3.0 s) to 1.32×10^4 (at 5.0 after heating) as the average surface temperature increases. Though the change in the value of $(Ma/Gr)_{\text{avg}}$ is small, it shows the trend that the buoyancy effects keep increasing as heat continues but in the 5 s of drop time they are still negligible.

The average Marangoni number is found to increase with time— 6.43×10^4 (at 3.0 s) to 1.66×10^5 (at 5.0 s after heating)—which means the free surface boundary layer does not reach steady state in 5 s of reduced gravity period and the flow is still developing. The free surface boundary layer steady state could not be achieved in 2.81 s, as estimated from an order-of-magnitude analysis because of the reverse flow created by the side walls, which was not considered in the order-of-magnitude analysis. Moreover, in the order-of-magnitude analysis the effect of heat transfer through the boundaries and vaporization of liquid from the free surface

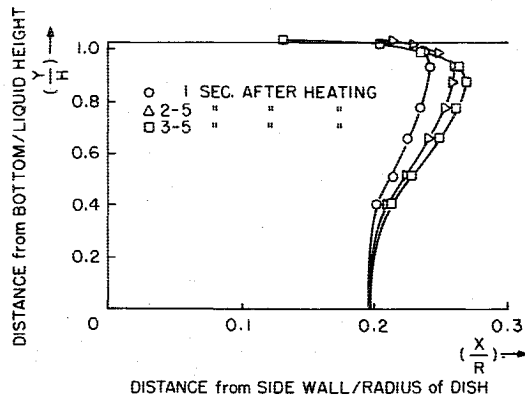


Fig. 7 Dye displacement with time—reduced gravity.

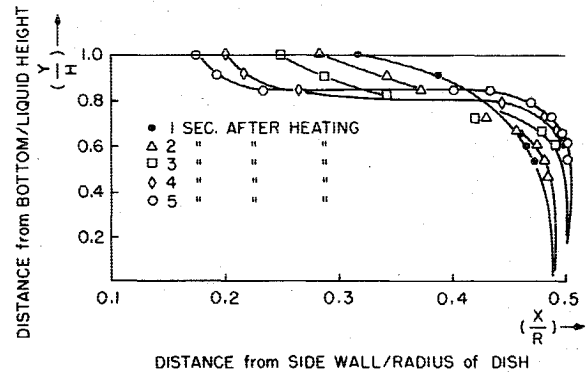
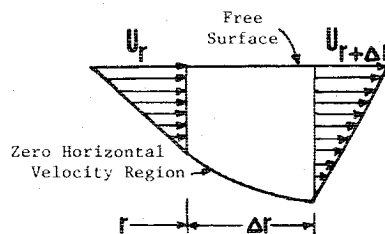


Fig. 9 Dye displacement with time—normal gravity.

Fig. 8 Schematic of fluid element inside the free surface.



are not considered though they are present in reality and affect the occurrence of steady state.

The two-way motion in the interior of the liquid and the decrease in surface velocities away from the heater can be explained as follows. The two-way motion in the interior of the liquid can be easily explained by means of continuity. If we consider that the free surface remains close to horizontal with time, as is observed in the tests, for mass conservation a given mass flow in one direction has to be compensated for by an equal mass flow in the opposite direction for a contained fluid. In order to understand the decrease in surface velocity with radius, we next look at the fluid element inside the free surface. Let us consider a fluid element of Δr thickness, at a distance r from the center and located between the free surface and the zero horizontal velocity region, as shown in Fig. 8. The zero horizontal velocity region is created by the appearance of the two-way flow as mentioned previously. The depth of the zero velocity region from the free surface is L_r and $L_r + \Delta r$, and the free surface velocities are U_r and $U_r + \Delta r$, at a distance of r and $r + \Delta r$ from the center, respectively.

Assuming small vertical velocities in the region, as has been found in the order-of-magnitude analysis, we obtain a relation between U_r and $U_r + \Delta r$ using mass continuity:

$$2\pi(U_r)(L_r) = 2\pi(r + \Delta r)(U_r + \Delta r)(L_r + \Delta r) \quad (1a)$$

$$U_r + \Delta r = \left(\frac{r}{r + \Delta r}\right) \left(\frac{L_r}{L_r + \Delta r}\right) U_r \quad (1b)$$

It is observed from the experiments that the distance of the zero horizontal velocity region from the free surface increases as one goes away from the center because of the diffusion of momentum from the free surface to the interior of the liquid. So, $L_r + \Delta r > L_r$ for all r . Therefore, $U_r + \Delta r < U_r$. This shows that the continuity itself would lead to a decrease in surface velocity with radius, as is observed in Fig. 5.

Test 2

The free surface is preheated for 10 s before the drop. In the first 10 s during which the free surface is preheated at normal gravity, the surface motion away from the center is slower than that expected under reduced gravity conditions. As the

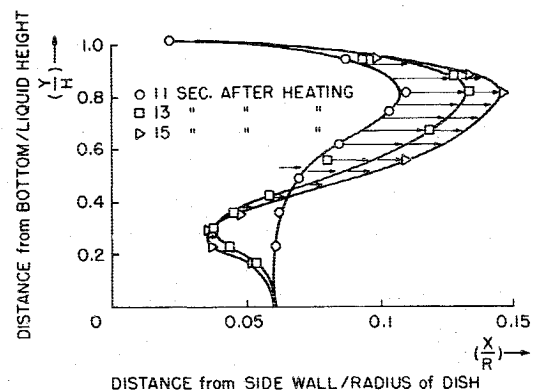


Fig. 10 Dye displacement with time—normal gravity.

experimental package enters the reduced gravity environment the surface velocities are seen to increase.

Comparing the temperature profiles in Figs. 4 and 11† we see that the temperature difference between the given points and at a given time are larger under normal gravity than in reduced gravity. This means that more heat is being transferred by convection under reduced gravity than in normal gravity because both of the tests are performed under identical initial conditions. This supports the aforementioned observation of higher surface velocities under reduced gravity.

Test 3

The free surface is preheated for 40 s before the drop so that a steady-state thermal boundary layer seems to be established during this preheat time under normal gravity environment. Except for the free surface effect, such as is observed in the preceding experiment (test 2), no change in the flow pattern is observed during the 5 s of reduced gravity. The two-way flow in the interior of the liquid remains the same.

The three experiments just described are repeated for identical initial conditions§ in a normal gravity environment. Dye displacement curves at different time intervals are given in Figs. 9 and 10. The temperature profiles for this case are presented in Fig. 11. The values of relevant dimensionless parameters are given in Table 1.

The temperature profiles up to 10 s after heating are drawn assuming the side wall temperature unchanged due to heating

†The temperature profiles in Fig. 10 are drawn as the mean temperature profiles over three runs. All of the temperature measurements are made by means of the thermistors and the temperature profiles are drawn assuming the surface temperature close to the side wall to remain the same as the initial liquid temperature for the first 5 s of heating. This is done to get some idea of the characteristic temperature difference.

§Initial conditions are heater wattage, liquid depth, initial liquid temperature.

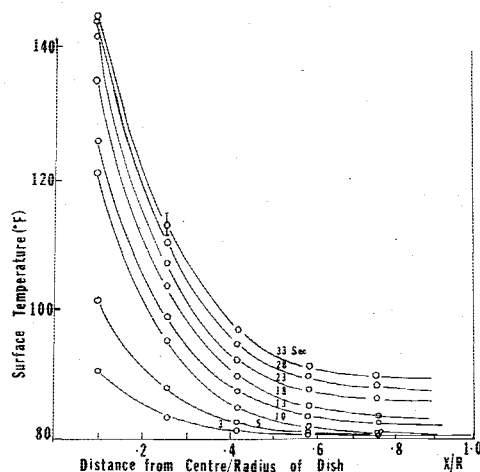


Fig. 11 Surface temperature profiles—normal gravity.

and are used to compare the results with the reduced gravity temperature profiles in Fig. 4. The temperature profiles between 10 s and 33 s after heating are used to get some idea of the temperature gradients present when the experimental package is dropped as in tests 2 and 3.

Comparison of the results (see Fig. 5) indicates that surface velocities are considerably higher under reduced gravity conditions than in normal gravity for same initial conditions. In Fig. 5 the normal gravity curve is drawn from a single run by tracking the dye particles as they move on the free surface. The velocities are calculated starting at 2.0 s after heating in a manner similar to the ones in the reduced gravity test 1. The velocities calculated between 2.0 and 4.0 s seem to remain the same.

It is observed that in the interior of the liquid the boundary layers near the free surface are thicker at 1 g than at reduced gravity. At normal gravity the Grashof numbers are found to be an order-of-magnitude larger than the Marangoni numbers, and so the flow due to density differences and buoyancy is dominant. This gives rise to large internal flows close to the free surface and directed away from the center of the dish. This flow is large close to the free surface because that is where the temperature gradients are present. But as heating continues, the heat diffuses downward and increases the Grashof number (see Table 1) and, ultimately, the mass flow, boundary-layer thickness, and internal velocities.

Thus, we see that though the free surface velocities are smaller, the overall mass flow rate away from the center is quite large due to the large density gradient induced flow. This gives rise to a large reverse flow due to continuity requirements.

Although none of the existing work (Refs. 1 to 4) deals with the identical configuration studied herein in that either the configuration or thermal boundary conditions are different and also it all deals with steady flows, the flow profiles (Figs. 7, 9, and 10) are qualitatively similar.

Conclusions

The present experiments have indicated that surface-tension gradients at reduced gravity can be dominant and can generate flows as large as buoyancy at normal gravity.

Under normal gravity the free surface can be said to be passive with respect to the heat-transfer process in the sense that the fluid motion is induced by buoyancy. The buoyancy effects are dominant in the form of a thicker free surface boundary layer produced by larger flow due to density gradients. Moreover, the free surface velocities at normal gravity are smaller than those under reduced gravity for the identical initial conditions.

As the gravity level is reduced ($10^{-5} g_0$) the surface tension gradient force becomes dominant ($Ma \sim 10^5$ and $Gr \approx 20$) and there is negligible gravity-induced convection. In this case, the free surface plays an active role in the heat-transfer process. Surface-tension gradient driven convection is seen to produce a thin boundary layer (~ 3.0 mm) near the free surface within a period of 5 s and a two-way flow is observed inside the liquid. Free surface velocities as high as $3.0 \text{ cm/s} \pm 0.1 \text{ cm/s}$ and internal velocities of the order of $1.0 \text{ mm/s} \pm 0.2 \text{ mm/s}$ in the reverse flow are observed. The foregoing velocities are obtained for the reduced gravity case with an 80-W heater.

Acknowledgment

This research was supported by NASA under Grant No. NSG-3053.

References

- Babitskiy, V. G., Sklovskiy, I. L., and Sklovskiy, Y. O., "Thermocapillary Convection in Weightless Conditions," *Space Studies in Ukraine*, No. 1, Space Materials Studies and Technology, 1973.
- Birikh, R. V., "Thermocapillary Convection in a Horizontal Layer of Liquid," *Journal of Applied Mechanics and Technical Physics*, Vol. 7, Jan. 1966, pp. 43-44.
- Levich, V. G., *Physicochemical Hydrodynamics*, Prentice Hall, Englewood Cliffs, N. J., 1962.
- Chia-Shun, Yih, "Fluid Motion Induced by Surface-Tension Variation," *The Physics of Fluids*, Vol. 11, March 1968, pp. 477-480.
- Grodzka, P. G. and Bannister, T. C., "Heat Flow and Convection Demonstration Experiments Aboard Apollo 14," *Science*, Vol. 176, May 1972, pp. 506-508.
- Pradhan, A. and Ostrach, S., "Surface-Tension Gradient Induced Convection Under Reduced Gravity Conditions," Case Western Reserve University, Cleveland, Ohio, FTAS/TR-76-123, 1976.